A 2.1-Mpixel Organic Film-Stacked RGB-IR Image Sensor With Electrically Controllable IR Sensitivity

Shin'ichi Machida, Sanshiro Shishido, Takeyoshi Tokuhara, Masaaki Yanagida, Takayoshi Yamada, Masumi Izuchi, Yoshiaki Sato, Yasuo Miyake, Manabu Nakata, Masashi Murakami, Mitsuru Harada, and Yasunori Inoue

***Abstract*— This paper describes an RGB-infrared (IR) organic CMOS image sensor with electrically controllable IR sensitivity. The sensitivities of all the pixels in the image sensor, which has the structure of two directly stacked organic layers with a high resistance ratio, are simultaneously controlled by changing the applied voltage to the organic films. The fabricated image sensor, with a pixel pitch of 3 μm, has 2.1 Mpixels (1920 × 1080) in both the RGB and IR regions. The sensor can switch between color imaging and IR imaging modes frame by frame without requiring a mechanically retractable IR-cut filter.**

***Index Terms*— CMOS image sensor, high resolution, IR image sensor, IR imaging, near infrared (IR), organic photoelectric conversion film (OPF), RGB-IR image sensor, wide dynamic range (WDR).**

I. Introduction

THE use of infrared (IR) imaging to view scenes that would otherwise be invisible to the human eye alongside visible-spectrum imaging is of interest to various fields of industry such as surveillance and machine vision. Conventional silicon image sensors with on-chip color filter arrays have IR sensitivity, because each color filter is transparent in the IR region as well as the corresponding color band. Therefore, mechanically retractable IR-cut filters have been adopted to image scenes in both color and IR. The IR-cut filter is inserted in front of the image sensor while capturing color images to achieve good color reproducibility, and the filter is removed when capturing IR images. However, the required increase in the number of mechanical components is undesirable for applications in which a small, lightweight, and highly robust system is necessary such as in vehicle or drone cameras.

Conventional RGB-IR image sensors without IR-cut filters have a specific color filter array that substitutes the IR pass filter for part of a Bayer arrangement [1], [2]. However, the loss of spatial resolution causes aliasing, as IR pixels are segmented within the effective pixel area. The 3-D stacking of photodiode arrays has been reported as a potential strategy for RGB-IR capture [3], but the need for bonding accuracy limits pixel size. Moreover, from the viewpoint of photoelectric conversion materials, silicon's weak IR light absorptivity results in a relatively low IR sensitivity in these image sensors.

Manuscript received April 28, 2017; revised July 28, 2017 and October 20, 2017; accepted October 20, 2017. Date of publication December 4, 2017; date of current version December 26, 2017. This paper was approved by Guest Editor Joseph Shor. *(Corresponding author: Shin'ichi Machida.)*

The authors are with the Advanced Research Division, Panasonic Corporation, Osaka 570-8501, Japan (e-mail: machida.shin-ichi@jp.panasonic.com).

Color versions of one or more of the figures in this paper are available online at http://ieeexplore.ieee.org.

Digital Object Identifier 10.1109/JSSC.2017.2769341

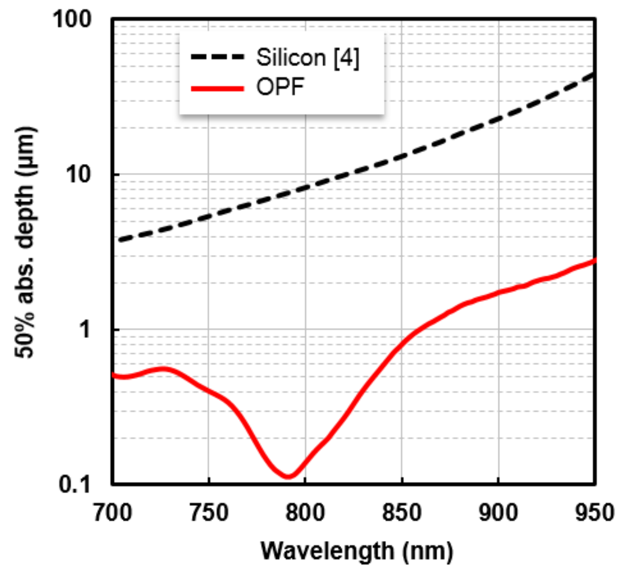

Fig. 1. 50% absorption depth with respect to wavelength.

Silicon requires a few micrometer or more of thickness to absorb 50% of the incident light in the IR region [4], as shown in Fig. 1. The deeper the photodiode portion is the more likely crosstalk is to occur. In contrast, organic photoelectric-conversion films (OPFs) can be thinned, typically to less than 1 μm, as organic materials are designed to sufficiently absorb at the desired wavelength. In this paper, an OPF that is sensitive to IR light is designed for use at a wavelength of 800 nm, and hence, a thickness of ∼100 nm is sufficient to absorb 50% of the incident light. Moreover, by stacking two OPFs, one sensitive to IR light and the other sensitive to visible light, an RGB-IR image sensor with full resolution for both visible light and IR light can be realized. An OPF stacking technique with TFTs and interlayer insulators has previously been reported [5]. However, patterned readout circuits increase the required number of control signal lines and readout lines in proportion to the number of stacked layers, which places limits on pixel size and number.

In order to solve the above-mentioned problems and to achieve an RGB-IR image sensor with high resolution and high sensitivity in the IR, we have adopted direct stacking of OPFs. This structure has only one readout line, even if multiple OPF

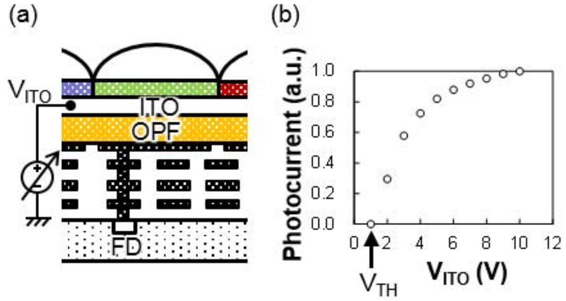

Fig. 2. (a) Cross-sectional schematic of an organic CMOS image sensor and (b) corresponding sensitivity.

layers are stacked. In this paper, a technique for controlling IR sensitivity, placing it in either the ON or OFF state is provided, and a 2.1-Mpixel RGB-IR image sensor with a 3-μm pixel size was successfully developed. This paper extends the work presented in [6] and provides additional circuitry details.

II. Direct OPF Stacking Structure for Waveband Controlling

Fig. 2 shows the cross-sectional schematic of an OPF image sensor and an example of the characteristic photocurrent as a function of the voltage applied to the indium tin oxide (ITO) electrode (V_{ITO}). The sensitivity depends on the voltage applied to the OPF, and hence, it is possible to control the global sensitivity by changing V_{ITO}. It should be noted that OPFs have a voltage threshold (V_{TH}) for extraction of photo-generated carriers. Only when V_{ITO} exceeds this threshold can photocurrent be collected by the floating diffusion (FD), while no charge can be extracted when the voltage is below the threshold. This characteristic enables an electrical global shutter function [7], [8], and also enables the sensor to switch between rolling shutter mode and global shutter mode. Because these thresholds are generally close among most OPFs, it is difficult to place the sensitivity of IR in the OFF state while maintaining the sensitivity for visible light if the visible-sensitive OPF and IR-sensitive OPF are simply stacked.

Our approach is based on the concept of a voltage dividing rule. If two OPFs are directly stacked, then the applied voltage is divided between each OPF depending on the resistance ratio, as shown in Fig. 3(a). The voltage for the IR-OPF (V_{IR}) is described by $V_{\text{IR}} = V_{\text{ITO}} \times R_{\text{IR}}/(R_{\text{RGB}} + R_{\text{IR}})$, where R_{IR} is resistance of the IR-OPF and R_{RGB} is that of the RGB-OPF, respectively. By designing the resistance ratio of those to be sufficiently large, it is possible to create a large difference between the voltages applied to the RGB-OPF and the IR-OPF. In other words, this allows the sensitivity of one OPF layer to be easily controlled across V_{TH} by changing V_{ITO}, which is supplied from the same voltage source. This is a result of the direct OPF stacking structure.

The photocurrent from the stacked OPF is the summation of that generated from the RGB-OPF and IR-OPF, as shown in Fig. 3(b) and (c). If the two OPFs are designed so that each resistance has a similar value ($R_{\text{IR}} \approx R_{\text{RGB}}$), the applied voltage is divided equally between each OPF and both V_{RGB} and V_{IR} exceed V_{TH} at the same V_{ITO}. In this case,

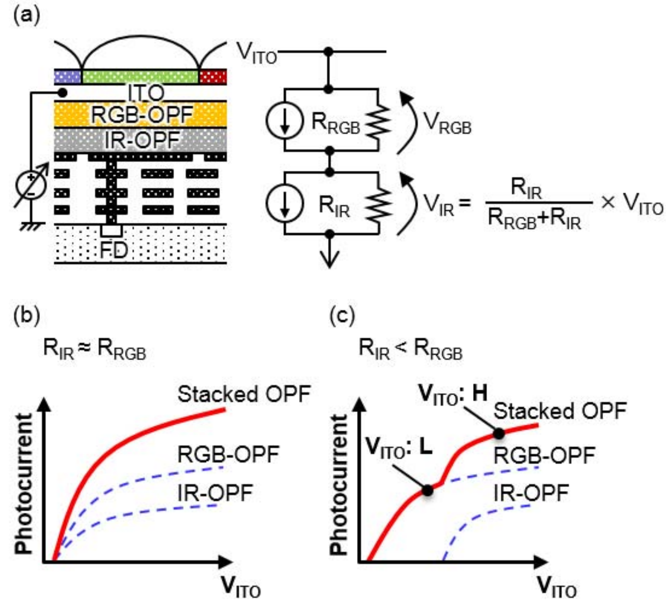

Fig. 3. Concept of direct OPF stacking structure. (a) Schematics of sensitivity in case of (b) $R_{\text{IR}} \approx R_{\text{RGB}}$ and (c) $R_{\text{IR}} < R_{\text{RGB}}$.

it is impossible to place the IR-OPF in the OFF state, while maintaining RGB-OPF in the ON state. On the other hand, if R_{IR} is designed to be smaller than R_{RGB} ($R_{\text{IR}} < R_{\text{RGB}}$), V_{IR} can be smaller than V_{RGB} at the given V_{ITO}. Therefore, the sensitivity of stacked OPF would have two thresholds with an increase of V_{ITO} as shown in Fig. 3(c). At a relatively low V_{ITO}, only RGB-OPF is ON state, while the IR-OPF is not sensitive to light because V_{IR} is below V_{TH}. At a relatively high V_{ITO}, both OPFs adopt the ON state. The sensitive waveband of the stacked OPF is limited to visible light at low V_{ITO} (RGB mode), and it expands to the IR region at high V_{ITO} (RGB + IR mode). This allows the IR sensitivity to be electrically controlled at any time, with a single readout line and using a common voltage source.

III. Chip Architecture

The pixel circuits and dual-column analog gain circuits are shown in Fig. 4. In order to achieve wide dynamic range (WDR) image capture, which is required to prevent saturation, dual-sensitivity pixels [9] have been adopted for the pixel structure. Each pixel has two cells with different aperture sizes and conversion gains, the larger pixel electrode cell for high sensitivity (CELL1) and the smaller pixel electrode cell for high saturation (CELL2), respectively. In the previous report on the dual cell structure [9], the pixel pitch was 6 μm and column comparators were provided for each of the two cells at 3-μm pitches. On the other hand, since the pixel pitch is reduced to 3 μm in this paper, it is structured to share one column comparator with two cells.

The noise reduction technique is an important subject, as correlated double sampling, a common technique in typical pinned photodiode pixels, cannot be used for absolute reset noise cancellation in organic CMOS image sensors. One of the solutions is to make use of a column feedback amplifier [10]. The chip architecture, we adopted uses basically the same

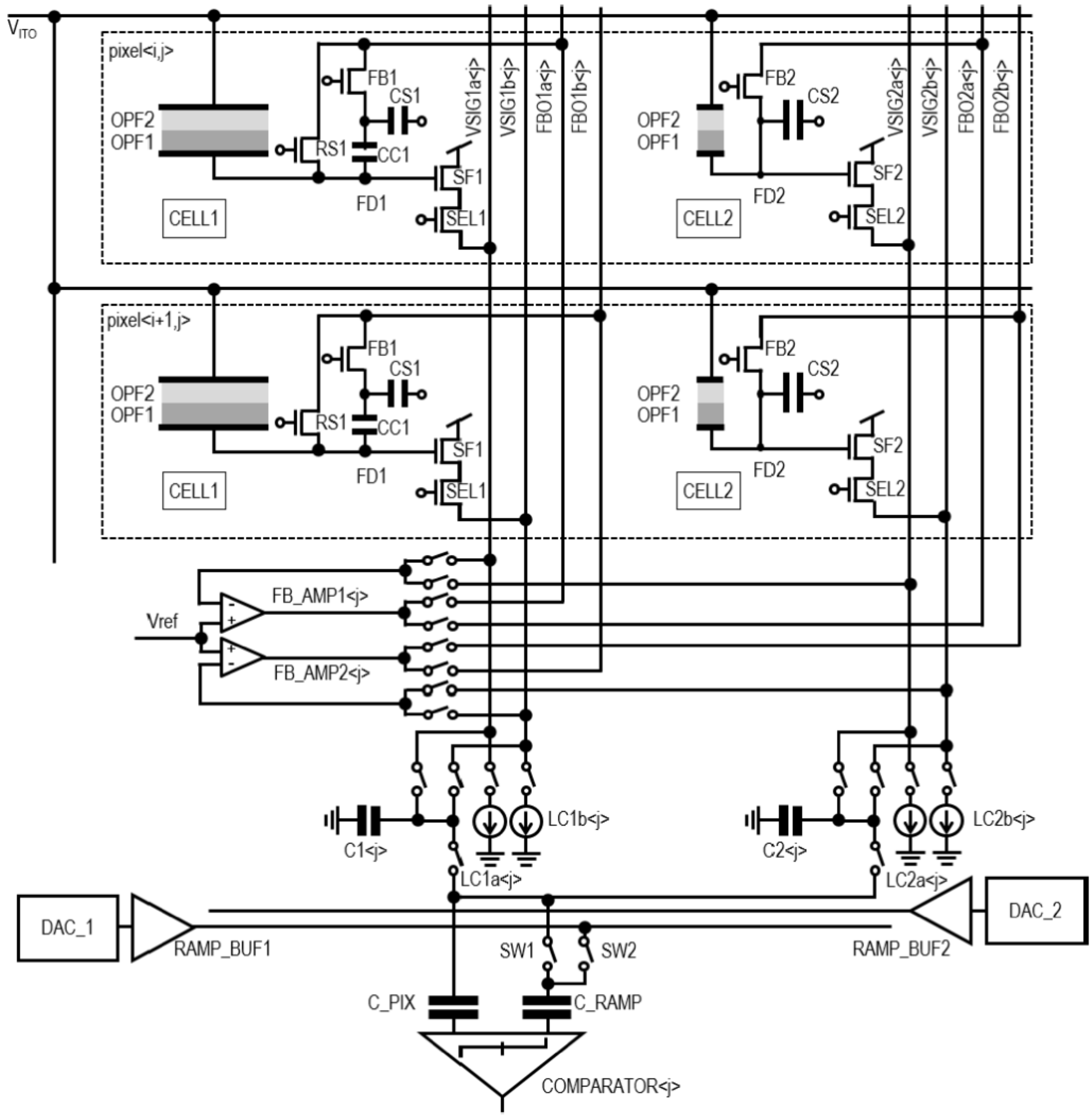

Fig. 4. Pixel architecture.

technique with the effect of noise reduction enhanced by the addition of a stabilized capacitor CS1 [9]. The reset noise of CELL1 can be suppressed by a factor of $1/\sqrt{(A \times CS1/CC1)}$, where A is gain of the feedback amplifier. The CS2, which is connected to the FD2 node, can enlarge dynamic range as it behaves as a charge-storage capacitor in CELL2. These in-pixel capacitors have metal–oxide–metal (MOM) structure and are located in the metal wiring layer, so that each pixel area can be shrunk to 3 μm despite increased integration density. The contribution to the noise reduction and dynamic range enlargement can be further enhanced by substituting high-k metal–insulator–metal capacitors for MOM capacitors [9].

The photo-generated carriers in OPFs are converted to a voltage and read by the in-pixel source follower SF1 or SF2, after which single-slope column analog-to-digital conversion (ADC) is executed at each column. In a certain exposure period the voltage of the pixel electrode, namely, the input of the source follower (SF), increases to nearly V_{ITO} at maximum in response to the photo-generated carriers. Signal charges are no longer accumulated after this saturation owing to an insufficient electric field in the OPF and the voltage range that SF can handle with linearity is defined by its supply voltage. As long as the sensor operates with a V_{ITO} higher than the supply voltage for the SF, saturation signal is defined independently by the value of V_{ITO}. In the case, that V_{ITO} is lower than the supply voltage is set; however, the amount of accumulated charges becomes peaked at V_{ITO}, leading to a decrease in saturation signal. Therefore, V_{ITO} should be selected to exceed the source voltage of SF in both RGB mode and RGB + IR mode in order for the sensor to work at full capacity.

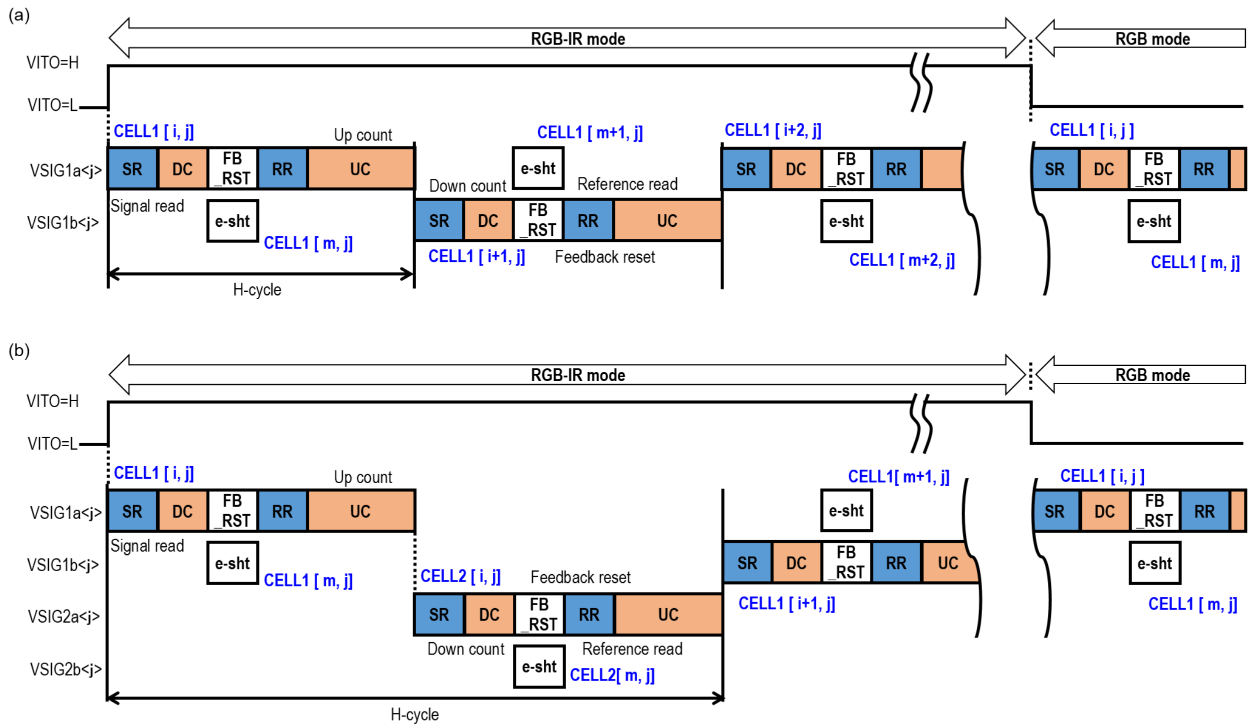

Fig. 5. (a) Timing chart of CELL1 read. (b) Timing chart of dual-cell read.

Fig. 5(a) shows a timing chart of CELL1 in the case of frame-by-frame switching between RGB + IR mode and RGB mode. At first, V_{ITO} is set to a relatively high (H) level for RGB + IR mode. During the signal read (SR) period, the signal value is read from CELL1[i, j] and is transferred to the input of ADC part through the signal line of VSIG1a. Then, during down count period, the signal value is converted to a digital value at the column comparator according to the single-slope ADC architecture. The FD level is then reset to the reference level through the reset transistor while suppressing kT/C noise using the feedback transistor [9] during the feedback reset (FB_RST) period. During the FB_RST period, electronic shutter (e-sht) operation is also conducted in another CELL1[m, j] through the VSIG1b line. In order to simultaneously execute reset operation and shutter operation, two different vertical signal lines, VSIG1a and VSIG1b, are alternately connected to pixels. During the reference read (RR) period, the reference level is read from CELL1[i, j] through VSIG1a and transferred to the input of ADC, followed by the conversion to digital value during the up count period. The signal output from CELL1[i, j] is determined as the difference between the two signal levels obtained during the SR and RR periods. Before moving to the next frame, V_{ITO} is changed to a relatively low (L) level for RGB mode. By means of these operations, visible images, including the IR spectrum and those excluding the IR spectrum, are obtained frame by frame.

Fig. 5(b) shows a timing chart of dual reading of CELL1 and CELL2 in an H-cycle for WDR imaging. Basic readout operation of CELL1 is the same as shown in Fig. 5(a). The main difference is that the read out operation of CELL2[i, j] is carried out before moving to the next row readout operation. CELL1[i, j] and CELL2[i, j] share one column comparator, therefore they are sequentially operated.

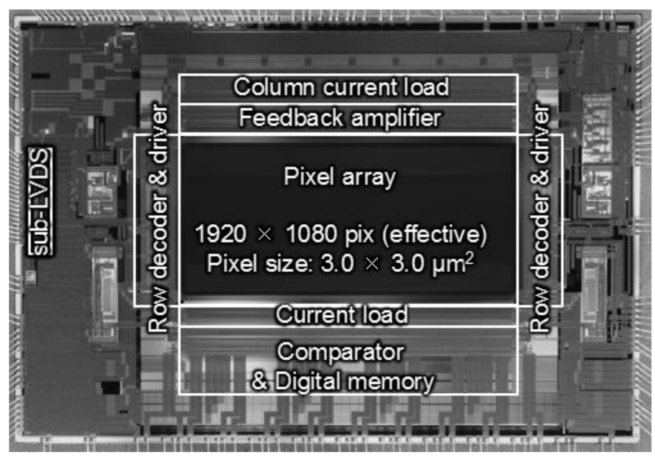

Fig. 6. Chip micrograph.

Fig. 6 shows a chip micrograph. The OPF image sensor was fabricated using a 65-nm 1P 3Cu 1Al CMOS process. Each pixel is 3-μm square and the pixel count is 1920 $\times$ 1080. On-chip micro lens and color filter array have not been implemented in this paper. A 12-bit single-slope ADC is implemented in each column, and the converted digital value is read out using a sub-LVDS buffer. The V_{ITO} is controlled with an off-chip driver.

IV. Experimental Results

Fig. 7 shows the relative sensitivity of the directly stacked OPFs as a function of wavelength. It is clear that the spectral

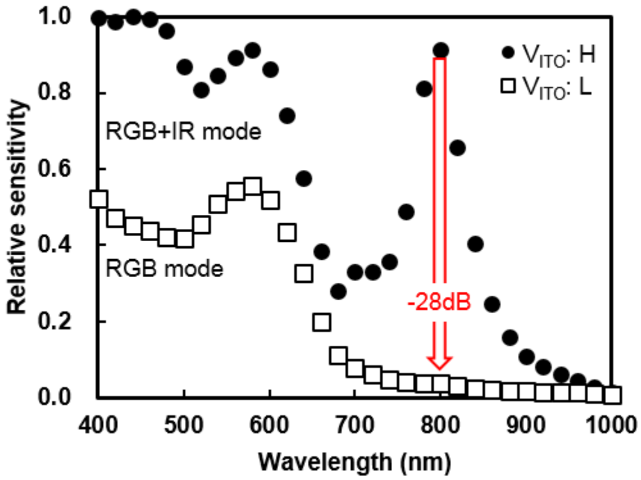

Fig. 7. Relative sensitivity of the fabricated image sensor.

Fig. 8. Captured images.

response varies depending on the V_{ITO}. At a high V_{ITO}, the sensitivity at a wavelength of 800 nm is as high as that in the visible spectral region, whereas at low V_{ITO}, the spectral sensitivity is lost beyond a wavelength of 700 nm. The extinction ratio of IR sensitivity at a wavelength of 800 nm is lower than −28 dB. Although, an on-chip RGB color filter array has not implemented at the present time, it will enable the image sensor to perform color imaging mode at low V_{ITO}, corresponding to RGB mode. This electrically controllable IR sensitivity thus enables one to switch from RGB + IR capture to RGB capture without the use of a mechanical IR-cut filter. Note that the wavelength providing the maximum sensitivity in the IR region can be tuned by varying the materials comprising the IR layer.

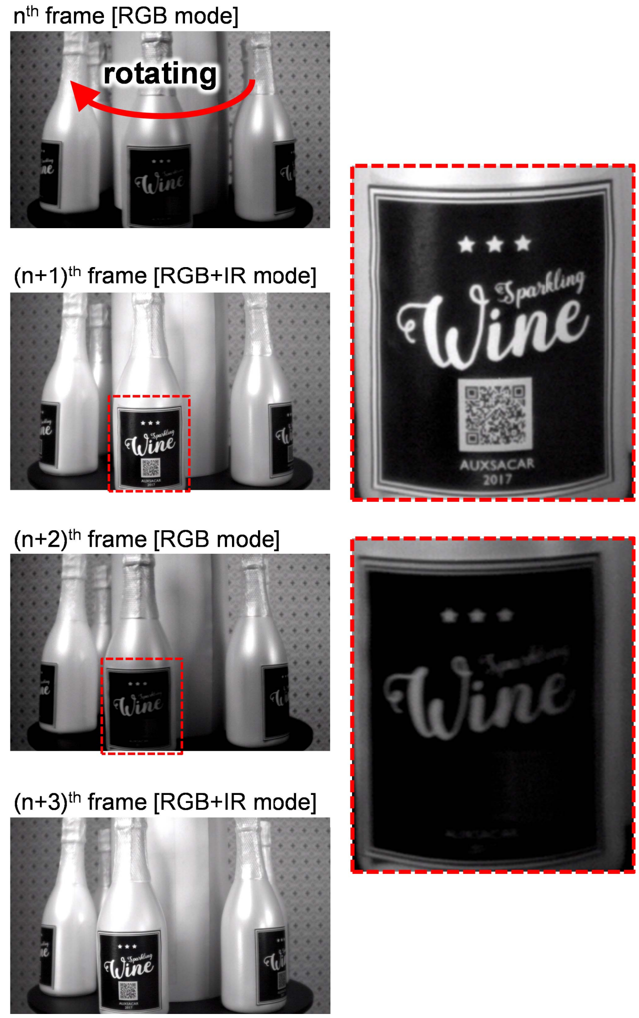

Fig. 9. Frame-by-frame capture.

The sensitivity to visible light in the RGB mode decreases to about half of that in the RGB + IR mode, which could be disadvantageous in RGB capture when compared to Si-based image sensors. This result suggests that the RGB-OPF is not sufficiently saturated in sensitivity under the bias condition of the RGB mode, differing from the concept shown in Fig. 3(c), as IR-OPF does not contribute to visible wavelength sensitivity. In other words, the resistance ratio could not be large enough for IR-OPF to maintain the OFF state before the sensitivity of RGB-OPF fully saturates. The resistance ratio depends on the materials and thickness of each OPF and can be affected by the intensity or wavelength of the incident light, and hence there is still room for optimization.

Images were successfully captured using the fabricated OPF image sensor, as shown in Fig. 8. The objects are illuminated with white LED light and IR LED light. All the images were captured with only CELL1, as shown in Fig. 5(a). Hence, WDR capture was not conducted. In the image captured with the RGB mode, it is hard to make out the objects behind the glass tank containing soy sauce, which transmits very little visible light. On the other hand, in the image captured with

TABLE I
SUMMARY OF SENSOR PERFORMANCE

Parameter	Value
Process technology	65 nm 1P 3Cu 1Al CMOS
Chip size	15.0 mm × 10.3 mm
Supply voltage	3.3 V
Number of effective pixels	1,920 (H) × 1,080 (V)
Pixel size	3.0 μm × 3.0 μm
Frame rate	60 fps
ADC architecture	single slope
ADC resolution	12 bit
Interface	sub-LVDS
Saturation signal	54,000 e^-
IR spectral range	700 nm to 940 nm
The maximum sensitivity wavelength in the IR region	800 nm
Extinction ratio of IR sensitivity	-28 dB (at 800 nm)

the RGB + IR mode, it is easy to identify the labels of the bottles behind the glass tank.

Since the spectral response depends on the V_{ITO}, the fluctuation of the voltage applied to each pixel can affect the image quality. Voltage drop by photocurrent or dark leakage current might cause brightness gradation, and non-uniformity of the ITO electrode may lead to sensitivity variation. The captured images show neither artificial gradation nor significant sensitivity variation, indicating the negligible effect of such fluctuations.

Furthermore, the IR sensitivity of this sensor can be electrically controlled at a speed of 100 μs or higher, which is much faster than the millisecond-order speed characteristics of mechanical shutters. By controlling the sensitivity of the image sensor electrically, frame-by-frame image capture of subjects in different spectra is realized, even though subjects move at high speed. This feature makes it possible to capture images in both visible light and IR light in alternate frames. Fig. 9 shows frame-by-frame images of bottles on a rotating table captured when RGB mode and RGB + IR mode are switched by changing V_{ITO}. The QR code on the bottle's label is printed with special ink reacting differently to different wavelengths. Even while rotating, the image sensor with IR sensitivity can capture a clear image of the QR code on the bottle's label. This feature can be applied to machine vision cameras for which both visual inspection and acquisition of invisible information are needed.

Table I summarizes the characteristics of the organic film-stacked RGB-IR image sensor. This fabricated sensor, with a pixel pitch of 3 μm, has 2.1-Mpixels in both the RGB and IR regions and exhibits maximum sensitivity at wavelength of 800 nm with spectral response from 700 to 940 nm in the RGB + IR mode. This wavelength selectivity, including maximum wavelength and spectral bandwidth, was derived from material properties of the IR-OPF, and should be tuned in order to suit a specific application. The future challenge will be how far we can extend the spectral response while maintaining high sensitivity. The residual IR sensitivity in the RGB mode, which relates to the extinction ratio of IR sensitivity, is also an important parameter for good color reproducibility. The sensor equipped with on-chip color filter array will be evaluated in order to examine image quality from this viewpoint.

V. CONCLUSION

We have successfully developed an organic CMOS image sensor whose waveband covers the visible to IR region. Introducing a direct OPF stacking structure based on a voltage dividing rule, global control of the IR sensitivity of the image sensor has been achieved by changing the voltage applied to the stacked OPFs. This technology enables one to capture both visual images, including color information and IR images, without the use of a mechanical IR-cut filter and has potential for use in viewing and sensing applications such as surveillance, non-destructive inspection, biometrics, and machine vision.

Conventional CMOS image sensors have made remarkable progress by fully exploiting the potential of silicon. However, it is desirable to develop new applications using invisible wavelengths for next-generation image sensors. With this in mind, the organic CMOS image sensor that utilizes the wavelength selectivity of materials has great appeal, and further technical evolution is expected in the future.

REFERENCES

[1] S. Koyama, Y. Inaba, M. Kasano, and T. Murata, "A day and night vision MOS imager with robust photonic-crystal-based RGB-and-IR," *IEEE Trans. Electron Devices*, vol. 55, no. 3, pp. 754–759, Mar. 2008.

[2] W. Kim *et al.*, "A 1.5 Mpixel RGBZ CMOS image sensor for simultaneous color and range image capture," in *IEEE Int. Solid-State Circuits Conf. (ISSCC) Dig. Tech. Papers*, Feb. 2012, pp. 392–393.

[3] Y. Takemoto *et al.*, "Multi-storied photodiode CMOS image sensor for multiband imaging with 3D technology," in *IEDM Tech. Dig.*, Dec. 2015, pp. 30.1.1–30.1.4.

[4] M. A. Green, "Self-consistent optical parameters of intrinsic silicon at 300 K including temperature coefficients," *Solar Energy Mater. Solar Cells*, vol. 92, no. 11, pp. 1305–1310, Nov. 2008.

[5] S. Aihara *et al.*, "Stacked image sensor with green- and red-sensitive organic photoconductive films applying zinc oxide thin-film transistors to a signal readout circuit," *IEEE Trans. Electron Devices*, vol. 56, no. 11, pp. 2570–2576, Nov. 2009.

[6] S. Machida *et al.*, "A 2.1 Mpixel organic-film stacked RGB-IR image sensor with electrically controllable IR sensitivity," in *IEEE Int. Solid-State Circuits Conf. (ISSCC) Dig. Tech. Papers*, Feb. 2017, pp. 78–79.

[7] M. Takase, Y. Miyake, T. Yamada, T. Tamaki, M. Murakami, and Y. Inoue, "First demonstration of 0.9 μm pixel global shutter operation by novel charge control in organic photoconductive film," in *IEDM Tech. Dig.*, Dec. 2016, pp. 30.2.1–30.2.4.

[8] S. Shishido *et al.*, "210ke- Saturation signal 3 μm-pixel variable-sensitivity global-shutter organic photoconductive image sensor for motion capture," in *IEEE Int. Solid-State Circuits Conf. (ISSCC) Dig. Tech. Papers*, Jan./Feb. 2016, pp. 112–113.

[9] K. Nishimura *et al.*, "An over 120 dB simultaneous-capture wide-dynamic-range 1.6e- ultra-low-reset-noise organic-photoconductive-film CMOS image sensor," in *IEEE Int. Solid-State Circuits Conf. (ISSCC) Dig. Tech. Papers*, Jan./Feb. 2016, pp. 110–111.

[10] M. Ishii *et al.*, "An ultra-low noise photoconductive film image sensor with a high-speed column feedback amplifier noise canceller," in *Proc. IEEE Symp. VLSI Circuits*, Jun. 2013, pp. 8–9.

Shin'ichi Machida received the B.S. degree in electrical and electronics engineering and the M.S. and Ph.D. degrees in nanomaterial science from Chiba University, Chiba, Japan, in 2008, 2010, and 2013, respectively.

In 2013, he joined Panasonic Corporation, Osaka, Japan, where he has been involved in developing materials and device structures of organic CMOS image sensors.

Sanshiro Shishido received the B.S. degree in electrical and electronic engineering from Ritsumeikan University, Kyoto, Japan, in 2006, and the M.S. and Ph.D. degrees in materials science from the Nara Institute of Science and Technology, Ikoma, Japan, in 2008 and 2011, respectively.

In 2011, he joined Panasonic Corporation, Osaka, Japan, where he is involved in the circuit designing of organic CMOS image sensors.

Takeyoshi Tokuhara received the B.S. and M.S. degrees in electrical engineering from The University of Tokyo, Tokyo, Japan, in 2011 and 2013, respectively.

In 2013, he joined Panasonic Corporation, Osaka, Japan, where he has been involved in the research and development of organic CMOS image sensors.

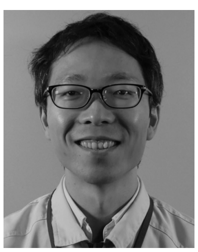

Masaaki Yanagida received the B.S. degree in electrical and electronics engineering and the M.S. degree in electrical engineering from Hosei University, Tokyo, Japan, in 2008 and 2010, respectively.

In 2010, he joined Panasonic Corporation, Osaka, Japan, where he is involved in developing sensor circuits and device structures of CMOS image sensors.

Takayoshi Yamada received the B.S. and M.S. degrees in mechanical engineering from Kobe University, Kobe, Japan, in 1993 and 1997, respectively.

In 1997, he joined Panasonic Corporation, Osaka, Japan, where he is involved in the development of device structures of organic CMOS image sensors.

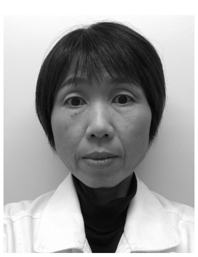

Masumi Izuchi joined Panasonic Corporation, Osaka, Japan, in 1983, where she is involved in the development of organic CMOS image sensors.

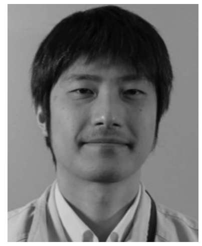

Yoshiaki Sato received the B.S. and M.S. degrees in computer science and electrical engineering from Kumamoto University, Kumamoto, Japan, in 2007 and 2009, respectively.

In 2009, he joined Panasonic Corporation, Osaka, Japan, where he is involved in the development of CMOS image sensor and organic CMOS image sensors.

Yasuo Miyake received the B.S. and M.S. degrees in electrical and electronic engineering from the Toyohashi University of Technology, Toyohashi, Japan, in 2005 and 2007, respectively.

In 2007, he joined Panasonic Corporation, Osaka, Japan, where he has been involved in CMOS image sensors. He is currently involved in the development of organic CMOS image sensors.

Manabu Nakata received the B.S. and M.S. degrees in electrical engineering from Doshisha University, Kyoto, Japan, in 2003 and 2005, respectively, and the Ph.D. degree in material chemistry from Kyushu University, Fukuoka, Japan, in 2013.

In 2012, he joined the Panasonic Corporation, Osaka, Japan, where he has been involved in the development of organic semiconductor devices.

Masashi Murakmi received the M.S. degree in electronic engineering from Doshisha Univeristy, Kyoto, Japan, in 1999.

Since 1999, he has been with Panasonic Corporation, Osaka, Japan, focusing on CMOS image sensor for 18 years. He is currently a Manager responsible for circuit design and device technology of organic CMOS image sensors.

Mitsuru Harada received the B.S. and M.S. degrees in materials development engineering from the Nagaoka University of Technology, Nagaoka, Japan, in 1989 and 1991, respectively.

In 1991, he joined Panasonic Corporation, Osaka, Japan. He is currently a Manager responsible for organic materials design of organic CMOS image sensors.

Yasunori Inoue received the B.S. and M.S. degrees in metallurgy from Kyoto University, Kyoto, Japan, in 1983 and 1985, respectively, and the Ph.D. degree in electronics and information systems engineering from Gifu University, Gifu, Japan, in 2002.

In 1985, he joined Sanyo Electric Co. Ltd., Osaka, Japan, where he has been involved in the development of CMOS SoC process and device technologies. He is currently a General Manager with Panasonic Corporation, Osaka, leading the development of organic CMOS image sensors.